Environmental effects on tilt measurements at Merapi volcano

Malte Westerhaus[1] *& Wolfgang Welle*[2]

[1]Geodetic Institute, Karlsruhe University, Englerstr. 7, D-76128 Karlsruhe

[2]GeoForschungsZentrum Potsdam, Telegrafenberg, D- 14473 Potsdam

1. Introduction

Deformations of the volcano's edifice due to pressure changes within the internal system of magma chambers and conduits are among the most important volcanic activity parameters. A wide spectrum of instruments and techniques is applied, including spaceborne as well as ground based measurements. Electronic tiltmeters, belonging to the latter group, are widely used if deformations are to be observed continuously. This type of instruments is robust, cheap and capable to monitor local deformations with a resolution of $\sim10^{-8}$ rad. As was shown by Rebscher at al. (2000) this resolution is high enough to clearly resolve earth tidal peaks. Due to the short base length of less than one meter, tiltmeter records are usually dominated by signals with a short wavelength, generated by nearby cracks and the local topography. Also, the response functions of tiltmeters to environmental disturbances (rain, temperature) may vary considerably from place to place. Effects of local geology may be recognized by combining several instruments in clusters with a side length of ~100 m, and meteorological disturbances are reduced by installing the sensors in bore holes or underground cavities. Insulating measures, however, cannot suppress tilt disturbances if the environmental noise source induces poro-elastic or thermo-elastic deformations of the ground. These signals that must be recorded by a sensitive tiltmeter coupled to the ground may fake or mask signals of volcanic origin. At Merapi Volcano, the situation is aggravated since heavy rain falls occasionally may be able to trigger pyroclastic flows (Purbawinata et al., 1997) that are expected to be accompanied by short term pressure fluctuations within the conduit. Any attempt to relate anomalous tilts to these eruptions (fig. 1) can only be successful if the possible influence of environmentally induced local/regional poro-elastic deformations is accounted for and if suspicious signals are removed from the individual records (as long as deformations of volcanic origin are of the same order of magnitude as the rain induced signals which is the case here). In the following, we will present some simplistic models of rain induced noise in tilt time series recorded at the flanks of Merapi Volcano.

2. The Indonesian-German deformation experiment

Merapi Volcano (2961 m) is located in Central Java, Indonesia (7.45° S, 110.44° E) at the subduction zone between the Eurasian and the Indo-Australian plate. Being one of the most active volcanoes in the world, Merapi has been elected into the list of the 16 so-called Decade Volcanoes. In 1995, the interdisciplinary research project MERAPI (Mechanism Evaluation, Risk Assessment, Prediction Improvement), a cooperation between the Volcanological Survey of Indonesia, the GeoForschungsZentrum Potsdam, and several institutes in Indonesia and Germany, started to investigate Merapi Volcano under different kinds of geophysical, geological and geochemical aspects (Zschau et al., 1998). The Indonesian-German deformation experiment carried out in the frame of MERAPI runs four continuously operating monitoring stations located at the flanks of the volcano at altitudes between 1280 m and 2020 m. Each station consists of one GPS receiver and an array of 3 electronic tiltmeters. Parallel to the deformation components, local environmental parameters (incl. rain, air- and soil temperature) are being recorded (Westerhaus et al., 1998). In contrast to other international groups monitoring tilt at Merapi Volcano, tiltmeters observing inclinations of a vertical ground element are used. They are based on electrolytical sensors in 2 orthogonal directions, with a specified accuracy of 0.1 mrad [Applied Geomechanics, 1991] and an effective accuracy of ~ 0.01 mrad. The vertical design of the tiltmeters allows an installation in boreholes at depths of 3 m to 4 m in order to minimize meteorological noise, especially the influence of temperature variations.

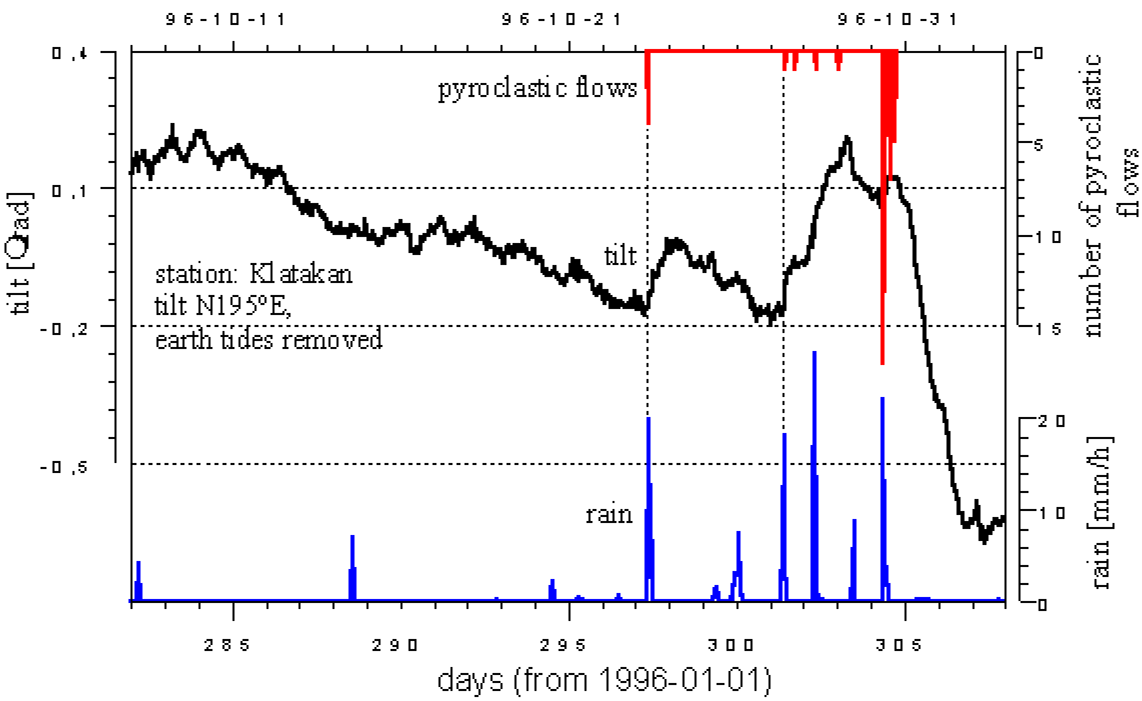

Figure 1: Rain water intruding into fractures of Merapi's active lava dome is apparently capable to trigger explosive eruptions, if the dome is in an unstable condition. Tilt anomalies accompanying the volcanic crisis have to be carefully checked with respect to rain-induced disturbances due to local poro-elastic ground deformation.

Most tiltmeters operated by other international research groups are installed at the summit of Merapi Volcano, close to the active lava dome. At those places strong tilt anomalies of the order of several hundreds of mrad are observed during phases of volcanic activity. Mostly, these signals result from finite block rotations caused by the growing lava dome and can hardly be inverted with respect to internal pressure changes. To our opinion, this is possible only from locations at the hillsides, far away from the secondary dome growing effects. On the other side, this opportunity has to be paid by much smaller signals. Up to now, tilt anomalies that are supposed to be of volcanic origin are as small as 1 mrad; the accompanying horizontal displacements are expected to be significantly less than 1 mm (Körner, 2000). Rain induced disturbances are up to 5 mrad on a time scale of days (fig. 4) and up to 25 mrad for the annual alternation of dry and wet seasons. Variations of similar size are observed elsewhere indicating that this magnitude of the rain induced disturbances is not unusual for shallow borehole installations (Kümpel, priv. comm.).

3. Ground deformation induced by rain

The total effect of rain on the tiltmeter installations is a combination of ground loading, i.e. normal compression and shearing of the ground down to the valley due to the added mass of water, and deformations of the soil matrix by movements of water through the pore space. Whereas the tilt reaction on the first effect is instantaneous, the diffusional character of the latter leads to a delayed response of the tiltmeters.

3.1. The loading effect

Fig. 2 shows a three month tilt record from a site (KEN, 1450 m, SE-flank) that is dominated by the loading effect. Negative radial tilt occurs as an instantaneous response to precipitation. The negative sign indicates a down-slope tilting of the top of the tiltmeter, compatible with a shearing of the ground down to the valley. Every negative tilt change is followed by an asymptotic movement in the direction back to the level before, giving a less rapid, positive tilt signal. Under conditions of uniaxial strain the instantaneous response of a tiltmeter to elastic loading of a half-space with a uniformly sloping surface is:

$$\Delta\varphi_l = \rho_w g \, \Delta h \sin\alpha \cos^2\alpha \frac{1}{\rho}\left(\frac{1}{v_s^2} - \frac{1}{v_p^2}\right) \qquad (1)$$

with Dj_l = instantaneous tilt effect, r_w = density of water, g = gravitational acceleration, Dh = height of the water column, a = slope, r = density of the soil, v_s and v_p = velocity of shear- and longitudinal waves in the upper soil layers, respectively. Inserting observed values of $a = 20^o$, v_p=850 m/s (Maercklin et al., 2000) and reasonable values of r = 1600 kg/m^3 and v_s = 300 m/s (equivalent to a Poisson's ratio v = 0.43), an instantaneous rain-tilt coupling coefficient of 0.018 mrad/mm is calculated.

$$f_i = \sum_{k=1}^{i} r_k e^{-(t_i - t_k)/\tau} \qquad (2)$$

The added water mass is removed from the surface due to overland flow, evapo-transpiration and diffusion to deeper soil layers, resulting in a gradual recovery of the tilt signal. The total loading effect is qualitatively described by a convolution of the rain data by an exponential function (e.g. Langbein, 1990):

where r_k is the amount of rain recorded at time t_k, t is a time constant and f_i is the cumulative effect of all the rain previous to t_k.

The resulting rain function (fig. 2) shows an instantaneous response to every rain event followed by an exponential decay which corresponds to the removal of water from the ground surface. A linear fit of the rain function to the data gives a local rain-tilt coupling coefficient of 0.023 mrad/mm (fig. 3b). This value is 28% larger than the theoretical rain-tilt admittance as calculated above. However, the variability of the soil parameters, especially if direct determinations are missing (r and v_s), may be at least as large as this difference. We, thus, conclude that the loading model is reasonable.

By subtracting the rain function f, the rain induced tilts are almost completely removed from the tilt series, with two exceptions on Aug.10, and Oct. 31 (figs. 2, 3). In both cases of apparently failed corrections heavy rainfalls coincided with pyroclastic flows, implying that a volcanic effect might be responsible for the residual tilt anomaly. However, the strong and unusual drift in the corrected tilt data, as observed after Oct. 31 (fig. 2), occurs again during the wet season one year later. Thus, the influence of rain on tilt at Kendil may not be explained completely by ground loading. As for other stations, poro-elastic deformations due to rain water infiltrating into the soil may be present, at least on an annual time scale.

3.2. The infiltration effect

The infiltration effect consists of two parts: (i) expansion of the upper soil layers due to increased pore pressure if water fills up formerly unsaturated pore space, and (ii) deformation of the soil matrix due to frictional resistance to flow of water. Expansion of the soil layers generates a tilt of a vertical element:

$$\Delta\varphi_p = \frac{1}{6}\frac{1+\nu}{1-\nu}(c-c_s)\sin 2\alpha\,\Delta p(z,t) \qquad (3)$$

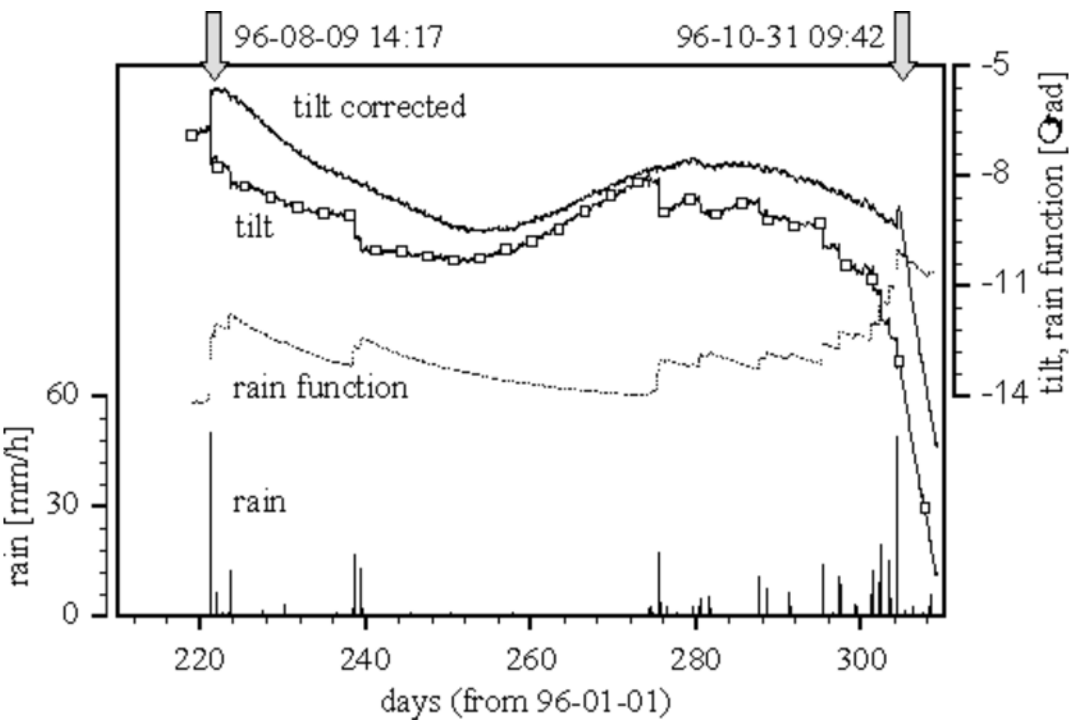

Figure 2: Illustration of the loading effect. The rain function has been calculated according to eq. (2) with *t* = 15 days. The tilt component is oriented parallel to the local slope; negative tilts indicate a down-slope tilting of the top of the tiltmeter. Arrows mark volcanic events.

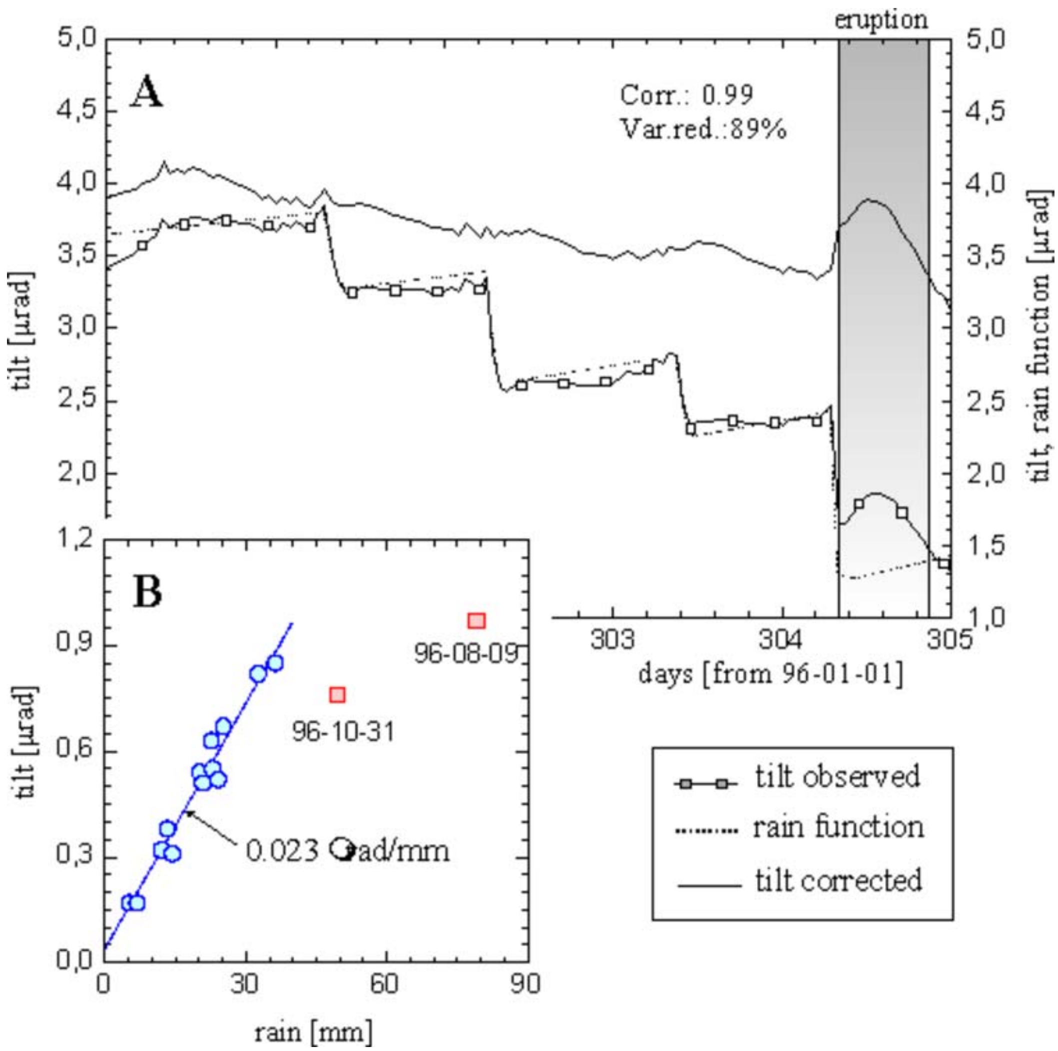

Figure 3: (A) days 300-305 of the timeseries shown in fig. 2; (B) linear regression between instantaneous tilt and rain (i.e. the steps in the tilt and in the rain function *f*). Values during phases of volcanic activity (rectangles) deviate considerably from the straight regression line. (A) shows the residual anomaly on Oct. 31, 1996, after subtracting the rain function from tilt according to the coupling coefficient 0.023 mrad/mm.

with D*jp* = delayed tilt anomaly due to pore pressure increase; *n* = Poisson's ratio; *c* = compressibility of the soil matrix; c_s = compressibility of the grains; *Dp* = pore pressure variation. *Dp* now is a function of depth *z* and time *t*, since the fluid needs time to diffuse through the pore space. Eq. (3) follows from the stress-strain relation under conditions of uniaxial strain analogous to the thermo-elastic tilt effect (e.g. Harrison and Herbst, 1977). With $c = 1*10^{-9}$ Pa, *n* = 0.43 and a soil porosity *F* = 0.5 the admittance between pore pressure and surface tilt amounts to *Djp* = 0.006 mrad/mm. As with the instantaneous effect, the sign is negative; i.e. increased pore pressure causes a down-slope tilting of the top of the tiltmeter. It should be mentioned that this model assumes 100% saturation. It can be shown that the high compressibility of gas bubbles would reduce the pore pressure immediately as soon as the volume fraction of gas in the pore space reaches approximately 1 part in 10^3 (Westerhaus, 1996). It seems well conceivable that such a small fraction of gas could be trapped in the pores during infiltration of rain water from above; in such a case expansion of the ground remains small and will contribute only marginally to the tilt disturbance.

$$\Delta\varphi_f = F(Ge, B, D, Q, z, t) \qquad (4)$$

The second effect is the result of pore fluid movements, driven by negative pressure gradients existing between the recharge and discharge areas. Friction between the mobile and immobile components of the soil leads to a deformation of the soil matrix. Kümpel et al. (1996) gave a comprehensive discussion of this mechanism for tiltmeters installed in the vicinity of pumped water wells. They showed that the resulting tilt anomaly:

is a function of the geometry, *Ge*, Skempton's parameter *B*, diffusivity *D*, discharge *Q* as well as space and time.

$$f_i = \sum_{k=1}^{i} \left(r_k - r_{k-1}\right) erfc\left(\frac{z}{2\sqrt{D\left(t_i - t_k\right)}}\right) \qquad (5)$$

Since most of the parameters entering eq. (4) are unknown, a quantitative calculation of the tilt disturbances is currently not possible. However, focusing on the diffusional character of the process we may be able to compute a rain function that qualitatively displays the time dependence of the deformations induced by the moving pore fluid. Neglecting the real geometry and assuming that a rain event generates a pore pressure disturbance at the surface of a semi-infinite half-space, pore pressure at depth z is governed by the complementary error function (see for example Turcotte & Schubert , 1982, pp 158, for the equivalent problem of heating or cooling of a semi-infinite half-space). The tilt effect may be described qualitatively by convolving the rain data by the complementary error function:

with erfc = complementary error function; *z* = depth (i.e. distance to the surface pressure disturbance; *D* = diffusivity. The approach assumes that the pore pressure disturbance at the surface consists of a series of Heavyside functions with the amplitudes (positive or negative) determined by the difference of two consecutive rain values. Each pressure step at the surface is continuated downwards by diffusion; pressure at depth *z* and time *t* is the cumulative effect of each previous step. In contrast to the exponential function the value of erfc at time $t_i = t_k$ is zero. Therefore, the response of the rain function to a rain event is not instantaneous but delayed; the maximum being reached after several days. Note, that no information about *z* and *D* is available; f_i is fitted to the observed tilt data by changing the ratio *z*/(2*sqrt(*D*)). The approach was successfully tested for the annual variations of soil temperature which is continuously monitored at each tilt station (in that case, depth z is known, and a reasonable guess of *D* is available from literature). Using air temperature as surface input in eq. (5), variations of the soil temperature are quantitatively predicted. Thermo-elastic effects in the tilt records are not obvious.

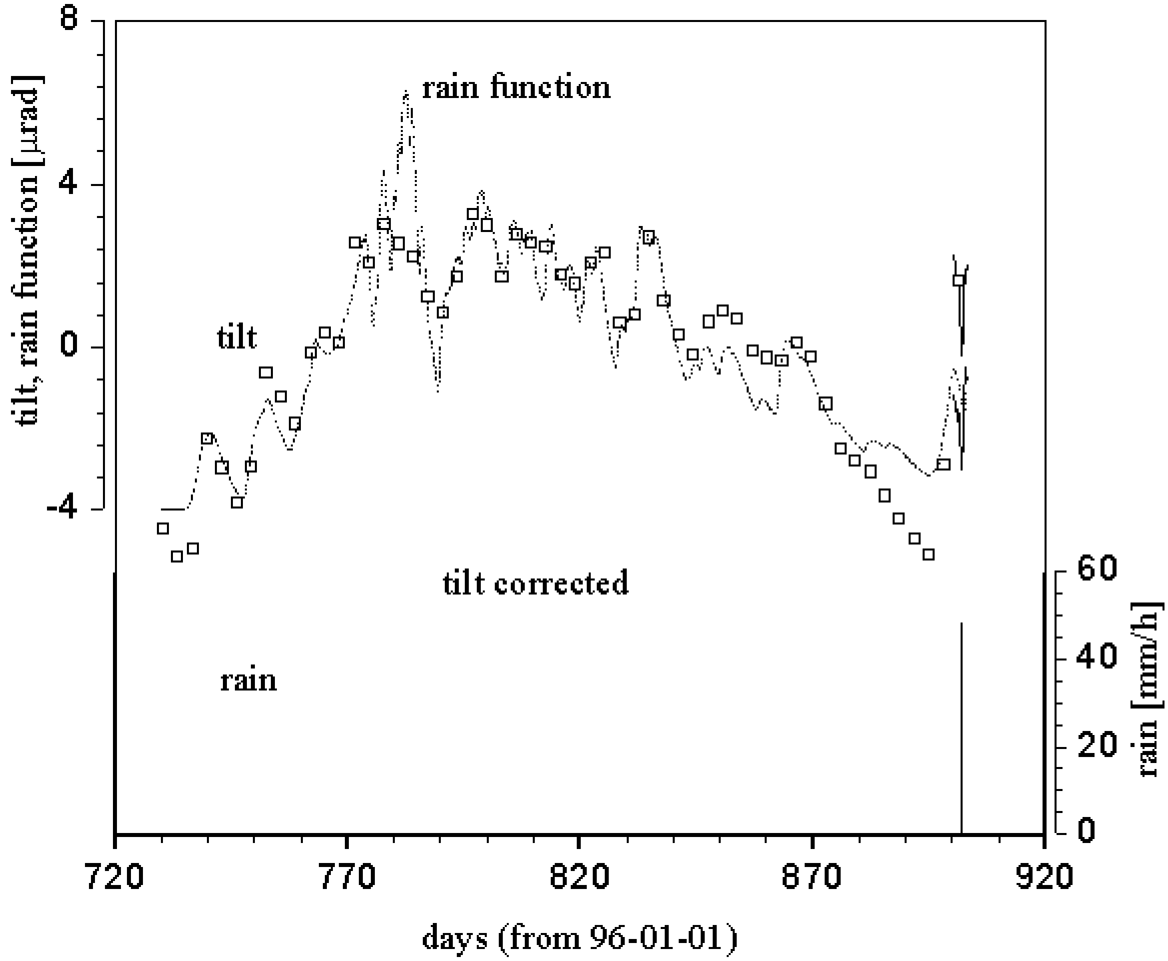

Figure 4: Illustration of the infiltration effect. The rain function has been calculated according to eq. (5) with z = 100 m, D varying linearly with pressure (fig. 5a) and soil retention (fig. 5b). The tilt component has been rotated in the direction of maximum rain influence (approx. parallel to the local slope).

The infiltration effect is nicely illustrated for site GEM (1380m) at the western flank of Merapi (fig. 4). The tilt record mirrors the rain function in almost any detail. As expected from eq. (5) the response of the tiltmeter to a rain event is delayed. An increase in the rain function causes a tilting of the top of the tiltmeter in the direction of the negative pore pressure gradient (the tilt curve in fig. 4 is rotated by 180^{o} for comparison). Although the comparison done in fig. 4 strongly suggests that the tilt record is dominated by the rain influence, the correlation is not perfect. The tilt residuals still exhibit short term variations of up to 5 mrad. The problem is that most hydraulic parameters like diffusivity, *D*, are a function of the saturation of the soil (e.g. Raudkivi & Callander, 1976, p. 25) resulting in a variable time shift between the tilt and rain function. To take this effect into account, diffusivity in eq. (4) was allowed to vary as a linear function of pore pressure (fig. 5a). Additionally, the limited capability of the soil to absorb water was accounted for by assuming an exponential model of soil retention (fig. 5b, see also Peters et al., 1991). These two assumptions improved the fit of the rain function to the tilt record fairly well. The variance reduction amounts to 83% with variable *D* and soil retention model, compared to 72% with constant *D* and no soil retention model.

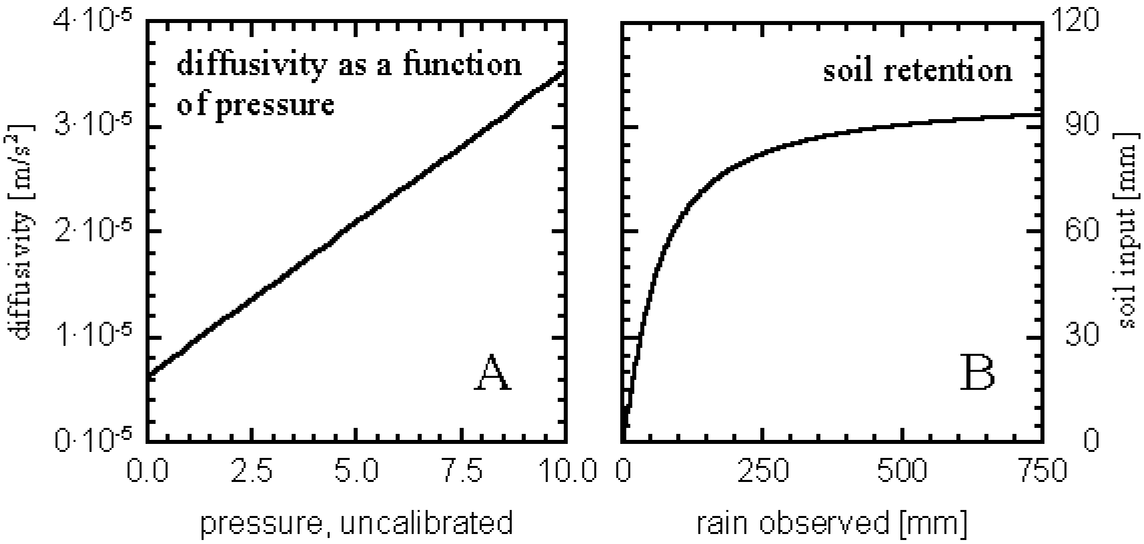

Figure 5: (A) assumed variation of diffusivity with fluid pressure; (B) model of soil retention. Note that the *D*-values in (A) are arbitrarily since the real geometry of the problem is not known (z=100 m chosen in eq. (5)).

The insufficient knowledge of the geometry of the problem and the time/saturation dependence of hydraulic soil parameters impedes an optimal fit of the rain function to the tilt data for time series longer than several weeks. This holds especially for the annual alternation of wet and dry seasons since the influence of soil retention becomes increasingly important with longer time periods. For short time segments, however, correction of the tilt records by subtracting an individually fitted rain function is capable to unravel 'interesting' signals by leaving only those tilt anomalies that are not induced by rain. These anomalies may then be investigated with respect to volcanic activity (fig. 6).

Conclusion

It is generally not possible to protect tiltmeters installed in shallow bore holes against real ground deformations that are induced by meteorological parameters like air pressure, air temperature and rain. It was shown that there are at least three ways for the rain to enter tilt observations: (1) compression of the ground by the added water mass, (2) expansion of the ground due to rising pore pressure with water infiltrating the soil, and (3) deformation of the soil matrix due to water flowing through the pore space. Mechanisms (1) and (2) are present in case of a sloping ground surface; mechanism (3) is invoked by horizontal pore pressure gradients. While (1) induces an instantaneous response of the tiltmeter that decays exponentially, (2) and (3) are governed by diffusion leading to a delayed response. The general response of a tiltmeter will be a combination of all three effects with their relative weights depending on the local conditions. The experience with the tiltmeter installations at the flanks of Merapi shows that usually infiltration of rain water into the ground is the predominant tilt generating process. The discussion of this process showed that it is not sufficient to just record precipitation. The amount of meteoric water observed at a location does give only the potential water input; it does not give sufficient information about the real changes in the soil water content. Thus, it is recommended to monitor the soil moisture directly. Replacing potential with the real soil water content in eq. (5) and considering effects of incomplete saturation will facilitate a more realistic modeling of the rain induced tilt disturbances.

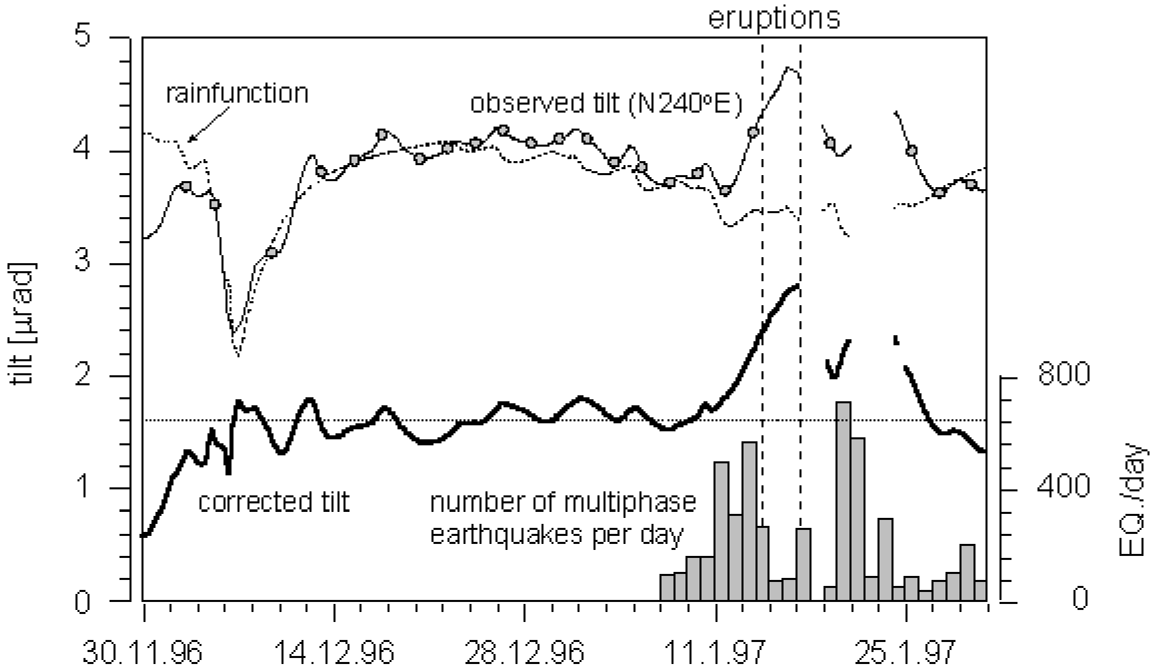

Figure 6: Fit of a rain function (eq. (5), constant *D*) to a 2-months tilt series at site KLT (1800m, W). After correction of rain induced disturbances a tilt anomaly during the volcanic crisis in January 1997 becomes clearly visible.

References

Applied Geomechanics, *Users's Manual*: Model 722 Borehole Tiltmeter, High Performance Option, Santa Cruz, USA, 20 pp, 1991.

Harrison, J. C. and Herbst, K. (1977). Thermoelastic strains and tilts revisited, *Geophys. Res. Lett.,* **4**, 535-537.

Körner, A. (2000). *Deformationsmodelle nach Auswertung von Tilmeter- und GPS-Daten für den Vulkan Merapi (Indonesien),* PhD-thesis, Universität Potsdam, 108 pp.

Kümpel, H.-J., Varga, P., Lehmann, K., and Mentes, Gy., (1996). Ground tilt induced by pumping - Preliminary results from the Nagycenk test site, Hungary, *Acta Geod. Geoph. Hung*., **31**, 67-79.

Langbein, J. O., Burford, R. O. and Slater, L. E. (1990). Variations in Fault Slip and Strain Accumulation at Parkfield, California: Initial Results Using Two-color Geodimeter Measurements, 1984-1988, *J. Geophys. Res.,* **95***:* 2533-2552, 1990.

Peters, G., Klopping, F. J. and Berstis, K. A. (1995). Observing and modelling gravity changes caused by soil moisture and groundwater table variations with superconducting gravimeters in Richmond, Florida, U.S.A., *Cahiers du Centre Europeen de Geodynamique et de Seismologie*, **11**, 147-159.

Purbawinata, M. A., Ratdomopurbo, A., Sinulingga, I. K., Sumarti, S. and Suharno (Ed.) (1997). *Merapi Volcano - A Guide Book,* Volcanological Survey of Indonesia, Bandung, Indonesia, 64 pp.

Raudkivi, A. J. and Callander, R. A. (1976). *Analysis of Groundwater Flow*, Arnold, London, 214 pp.

Rebscher, D., Westerhaus, M., Welle, W. and Nandaka, I. M. A. (2000). Monitoring ground deformation at the Decade Volcano Gunung Merapi, Indonesia, *Phys. Chem. Earth*, **25**, 755-757.

Turcotte, D. L. and Schubert, G. (1982). *Geodynamics*, John Wiley, New York, 450 pp.

Maercklin, N., Riedel, C., Rabbel, W., Wegler, U., Lühr, B.-G. and Zschau, J. (2000). Structural

Investigation of Mt. Merapi by an Active Seismic Experiment, In*: Deutsche Geophys. Gesellschaft - Mitteilungen*, Sonderband IV/2000, 13-16.

Westerhaus, M. (1996). *Tilt- and well level tides along an active fault*, Scientific Technical Report STR96/05, GFZ-Potsdam, 265 pp.

Westerhaus, M., Rebscher, D., Welle, W., Pfaff, A., Körner, A. and Nandaka, I.G.M. (1998): Deformation measurements at the Flanks of Merapi Volcano, *Deutsche Geophysikalische Gesellschaft, Mitteilungen,* Sonderband III/1998, 3-8.

Zschau, J., Sukhyar, R., Purbawinata, M. A., Lühr, B. and Westerhaus, M. (1998) Project *MERAPI* - Interdisciplinary Research at a High-Risk Volcano, *Deutsche Geophysikalische Gesellschaft, Mitteilungen,* Sonderband III/1998, 3-8.